Benzo[a]pyrene aggravated ovalbumin-induced epithelial tight junction disruption via ROS driven-NLRP3/Caspase-1 signaling pathway in asthmatic mice

YANQIU XU[1,2*], YANMING FENG[2*], LING WANG[2], XIN XU[1], LI XU[1] and BOHAN WANG[2]

[1]Nanjing University of Chinese Medicine, Nanjing, Jiangsu 210023, P.R. China; [2]Nanjing Jiangning Hospital of Chinese Medicine/Jiangning Chinese Medicine Hospital Affiliated to China Pharmaceutical University, Nanjing, Jiangsu 211100, P.R. China

Received February 19, 2025; Accepted May 22, 2025

DOI: 10.3892/ijmm.2025.5573

Abstract. Air pollutants contribute to the occurrence and development of asthma by impairing the airway epithelial barrier. However, underlying molecular mechanisms remain unknown. The present study investigated whether co-exposure to the air pollutant benzo[a]pyrene (BaP) and ovalbumin (OVA) enhanced OVA-induced epithelial tight junction disruption and explored the potential mechanisms involved. Asthma mouse and airway epithelial cell models were established and exposed to BaP. Lung pathology, immunoglobulin E (IgE), tight junction proteins zonula occludens-1 (ZO-1) and occludin, reactive oxygen species (ROS), NOD-like receptor protein 3 (NLRP3), apoptosis-associated speck-like protein containing a CARD, caspase-1, interleukin (IL)-18 and IL-1β were assessed by hematoxylin-eosin staining, enzyme-linked immunosorbent assay, western blotting, immunohistochemistry and immunofluorescence. Inhibitors of ROS and NLRP3 were used to assess their effect on ZO-1 and occludin and downstream signaling pathways to clarify BaP-induced damage. Lung tissue damage was exacerbated by BaP, the IgE level increased and the ZO-1 and occludin expression reduced in both models, thereby disrupting airway epithelial tight junctions. Additionally, BaP increased ROS levels and activated the NLRP3/caspase-1 signaling pathway. However, reducing ROS and NLRP3 restored the ZO-1 and occludin expression and improved epithelial integrity. Airway tight junction disruption was promoted by BaP by activating the ROS-driven NLRP3/caspase-1 signaling pathway.

Correspondence to: Dr Bohan Wang, Nanjing Jiangning Hospital of Chinese Medicine/Jiangning Chinese Medicine Hospital Affiliated to China Pharmaceutical University, 657 Tianyin Avenue, Jiangning, Nanjing, Jiangsu 211100, P.R. China
E-mail: jswbh2020@126.com

Dr Li Xu, Nanjing University of Chinese Medicine, 138 Xianlin Avenue, Qixia, Nanjing, Jiangsu 210023, P.R. China
E-mail: xlnjucm126@163.com

*Contributed equally

Key words: benzo[a]pyrene, asthma, airway epithelial cells, tight junction, NOD-like receptor protein 3/caspase-1 signaling pathway

Introduction

With the worsening of air pollution, diseases such as asthma, acute respiratory infections and lung cancer are becoming prevalent. Asthma is a heterogeneous disease characterized by chronic airway inflammation and progressive airway remodeling, with >350 million patients worldwide (1). Long-term exposure to air pollutants can increase the frequency of acute asthma attacks and worsen disease progression (2,3). Benzo[a]pyrene (BaP), the most toxic among the polycyclic aromatic hydrocarbons (PAHs), is a widespread atmospheric organic pollutant. Major sources include car emissions, tobacco smoke, cooking and industrial burning (4,5). Epidemiological studies reveal that BaP exposure is markedly associated with more frequent acute asthma attacks, reduced lung function and aggravated clinical symptoms (5,6). Choi *et al* (7) reported that children exhibited a high risk of asthma diagnosis after exposure to high BaP level. In animal studies, BaP, with allergen ovalbumin (OVA) and dust mite extract, can increase allergen-specific immunoglobulin E (IgE) level, systemic T-helper 1/2 (Th1/Th2) responses and airway inflammation (8). Although evidence continues to grow regarding the harmful effect of BaP on respiratory health, the precise molecular mechanism involved in lung toxicity remains unknown.

The airway epithelium serves as a first barrier against external allergens, pollutants and pathogens (9). Toxic substances in polluted air can stimulate and damage this barrier, contributing to the onset and progression of asthma. Disruption of the airway epithelial barrier not only increases susceptibility to respiratory infections and exacerbation but also exposes the underlying tissues to external agents, initiating inflammation, remodeling and heightened airway reactivity (10,11). Epithelial cells maintain barrier through tight junctions, which seal the gaps between cells and regulate the selective permeability (12,13). Occludin and zonula occludens-1 (ZO-1) are key proteins involved in tight junction regulation (14). The discovery of occludin as the first transmembrane protein associated with tight junctions identified it

as a crucial marker of barrier integrity (15). It plays a crucial role in stabilizing tight junctions and maintaining epithelial cohesion. Scaffolding protein-like function is performed by ZO-1, linking tight junction transmembrane proteins to the cytoskeleton and organizing the junction complex. Due to its central role, ZO-1 is widely used as a major marker for evaluating intercellular barrier function (16,17).

Elevated reactive oxygen species (ROS) production from air pollutant exposure is a key mechanism underlying airway epithelial barrier damage. Oxidative stress induced by ROS harms cell membranes and tight junction proteins, thereby reducing the integrity and functionality of the airway epithelium. As BaP is cytotoxic, mutagenic and highly lipophilic, it promotes oxidative damage by promoting ROS production (18). Increased ROS enhance epithelial permeability, while their reduction restores the expression of occludin and ZO-1 (19,20). However, the exact mechanism by which BaP-induced ROS production affects occludin and ZO-1 remains unclear. Reports indicate that the NOD-like receptor protein 3 (NLRP3) inflammasome disrupts the epithelial barrier and contributes to allergic airway inflammation, with ROS being essential for its activation (21). This suggests that BaP-induced ROS may activate the NLRP3 inflammasome and regulate occludin and ZO-1 expression in asthma. The present study used asthma mouse and epithelial cell models exposed to BaP to assess ROS level, NLRP3 activation and tight junction protein, aiming to clarify how BaP exacerbates asthma-related barrier damage via signaling pathways.

Materials and methods

Animal experimental design. A total of 48 specific-pathogen-free grade female BALB/c mice (6-8 weeks old, 18-22 g) were obtained from Beijing Sibeifu Biotechnology Co., Ltd. All procedures were approved by the Animal Ethics Committee of the Affiliated Hospital of Nanjing University of Traditional Chinese Medicine (approval no. 2022DW-48-02). All mice were housed with a standard temperature (20-24˚C) and humidity (50-60%), with a 12 h light/dark cycle. The standard feed used in the present study was purchased from Nanjing Yinuojia Feed Co., Ltd. and was composed of corn, wheat, imported fish meal, chicken meal, soybean meal, soybean oil, amino acids, vitamins and minerals. The production batch number was 24100108, which met Chinese national hygienic standard for formula feed for laboratory animals. After sterilization by irradiation, it met the hygienic requirements of SPF grade laboratory mice.

As described previously (22,23), an aggravated asthma model was established using OVA sensitization and challenge combined with BaP exposure. The 24 mice were divided into three groups (n=8/group): control, OVA and OVA + BaP groups. On days 0 and 14, mice in OVA and OVA + BaP groups received intraperitoneal injection of 100 μg OVA (MilliporeSigma) with potassium aluminum sulfate, followed by an intranasal administration of 50 μl OVA on days 14, 25, 26 and 27. Group OVA + BaP also received 50 μl of BaP (MilliporeSigma) solution (4 μg/per mouse) on days 14, 16, 18, 20, 22, 24 and 26. Control mice received normal saline using the same manner. Mice were fasted overnight before blood sample collection on the final day. The mice were euthanized by filling with carbon dioxide at the rate of 30% CO_2 tank volume/min.

Based on the initial results, a second batch of 24 mice were divided into 3 groups with 8 mice in each group. The temperature, light/dark cycle and humidity were the same as those of the first batch. The second batch of experiments was conducted using the same OVA + BaP and the control protocols. An additional group, OVA + BaP + NAC, received N-acetylcysteine (NAC) intragastrically at 250 mg/kg once daily from days 14 and 27, while other groups received 0.2 ml of normal saline.

Histological analysis. Left lung tissues were rinsed with phosphate-buffered saline (PBS), fixed in 4% formalin for 24 h at room temperature then dehydrated with graded alcohol, immersed the tissue in molten paraffin, forming wax blocks after cooling. Sections (4 μm thick) were dewaxed with xylene, rehydrated through gradient ethanol and stained with hematoxylin and eosin (5 min at room temperature). Tissue morphology was observed under a light microscope at x200 magnification.

ELISA. Mouse serum IgE levels were measured using an Anti-OVA IgE ELISA kit (Cayman Chemical Company; cat. no. 500840). Standards and samples were added to duplicate wells and incubated for 2 h at room temperature. Detection working solution of IgE was added and shaken at room temperature for 1 h. Streptavidin-conjugated horseradish peroxidase was then applied and incubated at room temperature for 30 min. After adding tetramethylbenzidine substrate solution, absorbance at 450 nm was measured using a microplate reader. The IgE level was determined using a standard curve.

Cell culture. Human bronchial epithelial (16HBE) cells, obtained from the Chinese Academy of Sciences (Shanghai, China), were cultured in Rosewell Park Memorial Institute (RPMI) 1640 medium (Gibco; Thermo Fisher Scientific, Inc.) supplemented with 10% fetal bovine serum (Biological Industries, Inc.) and 1% penicillin-streptomycin solution (Gibco; Thermo Fisher Scientific, Inc.). After the cells adhered, BaP was added at concentrations of 2.5, 5, 10 and 20 μM. Following BaP induction, NAC (10 mM; Beyotime Institute of Biotechnology) and MCC950 (10 μM; Selleck Chemicals) were administered for 48 h before sample collection.

ROS assay. Frozen sections of lung tissues were prepared and circled using a histochemical pen. A spontaneous fluorescence quenching agent was applied for 5 min, followed by a 10 min water rinse. A ROS dye solution was added and incubated for 30 min at 37˚C in the dark. The nuclei were counterstained with DAPI, followed by three washings with an anti-fluorescence quenching agent and capturing images after sealing the slides. In 16HBE cells, dichloro-dihydro-fluorescein diacetate (DCFH-DA; Nanjing Jiancheng Bioengineering Institute) was used to assay ROS levels and was diluted 1:1,000 in RPMI 1640 medium. Cells were incubated at 37˚C in 5% carbon dioxide for 30 min. After removing the medium and washing twice with PBS, images were captured under a fluorescence microscope.

Immunofluorescence staining. Paraffin-embedded lung tissue sections were deparaffinized and subjected to antigen retrieval in an ethylenediaminetetraacetic acid buffer. Immunol staining fix solution was used to fix 16HBE cells for 60 min at room temperature and permeabilized with Triton X-100 (Beyotime Institute of Biotechnology) in PBS. They were all blocked with 10% goat serum (Beyotime Institute of Biotechnology) for 60 min at room temperature. The lung tissues sections were incubated with anti-ZO-1 (1:200 dilution; cat. no. 21773-1-AP; Wuhan Sanying Biotechnology), anti-occludin (1:200 dilution; cat. no. 66378-1-Ig; Wuhan Sanying Biotechnology), anti-NLRP3, (1:200; cat. no. ab270449; Abcam), anti-apoptosis-associated speck-like protein containing a CARD (ASC; 1:200; cat. no. 67824T; CST) overnight at 4˚C. The 16HBE cells with a density of 70-80% were incubated with anti-ZO-1 (1:400 dilution; cat. no. 21773-1-AP; Wuhan Sanying Biotechnology), anti-occludin (1:400 dilution; cat. no. 66378-1-Ig; Wuhan Sanying Biotechnology) anti-NLRP3 (1:100; cat. no. WL02635; Wanleibio Co., Ltd.) and anti-ASC (1:200; cat. no. sc-514414; Santa Cruz Biotechnology, Inc.) overnight at 4˚C. On the following day, all samples were washed with PBS buffer and incubated with secondary antibodies (Wuhan Sanying Biotechnology) for 60 min at room temperature and stained with DAPI (Beyotime Institute of Biotechnology) for 5 min at room temperature. After applying anti-fluorescence quenching agents, images were acquired using a fluorescence microscope (Nikon Corporation).

Western blot analysis. Total proteins were extracted by radioimmunoprecipitation analysis lysis buffer. The protein concentration was determined with a bicinchoninic acid assay kit (Beyotime Institute of Biotechnology). Protein samples were mixed with the loading buffer at a 1:5 ratio and heated at 99˚C for 10 min to denature proteins. 20 μg of protein were separated using sodium dodecyl sulfate-polyacrylamide gel electrophoresis, with 10% separating and 5% stacking gel. After, proteins were transferred onto polyvinylidene difluoride membranes and blocked with 5% nonfat milk at room temperature for 1 h. Membranes were then incubated with primary antibodies [anti-ZO-1 (1:5,000; cat. no. 21773-1-AP; Wuhan Sanying Biotechnology), anti-occludin (1:5,000; cat. no. 66378-1-Ig; Wuhan Sanying Biotechnology), anti-NLRP3 (1:1,000; cat. no. WL02635; Wanleibio Co., Ltd.), anti-ASC (1:1,000; cat. no. 67824T; CST), anti-interleukin (IL)-18 (1:1,000; cat. no. A1115; ABclonal Biotech Co., Ltd.), anti-caspase1 (1:1,000; cat. no. WL03450; Wanleibio Co., Ltd.)] and anti-β-actin (1:5,000; cat. no. T0022; Affinity Biosciences) overnight at 4˚C. The membranes were incubated with HRP Goat anti rabbit IgG (1:8,000; cat. no. BA1054; BOSTER Biological Technology Co., Ltd) or HRP Goat anti mouse IgG (1:5,000; cat. no. BA1050; BOSTER Biological Technology Co., Ltd.) for 1 h at room temperature the next day., then visualized and analyzed using an enhanced chemiluminescent detection system and Image Lab software (BL520; Bio-Rad Laboratories, Inc.).

Statistical analysis. All data are expressed as mean ± standard deviation and GraphPad Prism software (version 10.0; Dotmatics) was used to make statistical graphs. Comparisons between two groups were performed using a unpaired t-test, while multiple group comparisons were performed using one-way analysis of variance followed by Tukey's post hoc test to analyze significant differences between groups. $P<0.05$ was considered to indicate a statistically significant difference.

Results

BaP can aggravate OVA-induced epithelial tight junction disruption in asthmatic mice. To assess the effect of BaP, an air pollutant, on airway epithelial tight junction, BALB/c mice were used. Asthma was induced with OVA, while an enhanced model was established using OVA + BaP. As demonstrated in Fig. 1A, control mice exhibited smooth bronchial walls and orderly epithelium. The OVA group revealed disordered epithelium and inflammatory cell infiltration. Co-exposure to BaP and OVA results in an increased in inflammatory cell infiltration, more pronounced tracheal wall fold, more severe epithelium disorganization and some epithelial cell loss. Serum IgE levels were markedly elevated in the OVA group compared with control and further increased in OVA + BaP (Fig. 1B). Tight junction proteins ZO-1 and occludin indicated intercellular barrier function. In OVA-treated lung tissue, occludin and ZO-1 levels were reduced compared with control and further decreased in the BaP + OVA group (Fig. 1C). Immunofluorescence results (Fig. 1D) followed this trend, indicating BaP could disrupt tight junctions by downregulating ZO-1 and occludin.

BaP can induce disruption of the tight junction of airway epithelial cells. 16HBE cells were treated with various BaP concentrations revealing reduced expression of tight junction markers. Western blot analysis (Fig. 2A) revealed reduced ZO-1 and occludin levels with increasing BaP dose. Immunofluorescence staining (Fig. 2B) revealed decreased ZO-1 (green) and occludin (red) fluorescence at 10 and 20 μM Bap, indicating reduced protein expression, while 2.5 and 5 μM revealed no significant change. These results suggested that BaP impaired tight junction integrity in a dose-dependent manner.

BaP induces NLRP3/caspase-1 pathway activation in lung tissue of asthmatic mice. Allergen-induced airway inflammation involves NLRP3 inflammasome activation. Previous studies report elevated NLRP3 in Ova-induced asthma (24,25), but the effects of BaP co-exposure remain unclear. Upon activation, NLRP3 converts procaspase-1 into caspase-1, leading to IL-1β and IL-18 maturation. Western blotting and immunofluorescence were used to detect inflammasome components. As revealed in Fig. 3A, NLRP3 and ASC expressions were higher in the OVA than control and further elevated in the OVA + BaP group. Additionally, fluorescence double staining revealed increased NLRP3 and ASC aggregation in the OVA + BaP group, indicating inflammasome activation. Exposure to BaP markedly increased NLRP3 and ASC expression, caspase-1, IL-18 and IL-1β levels compared with the control and OVA groups (Fig. 3B and C).

BaP activates the NLRP3/caspase-1 pathway in airway epithelial cells. As demonstrated in Fig. 4A, treatment with 10 and 20 μM BaP increased the fluorescence intensity of

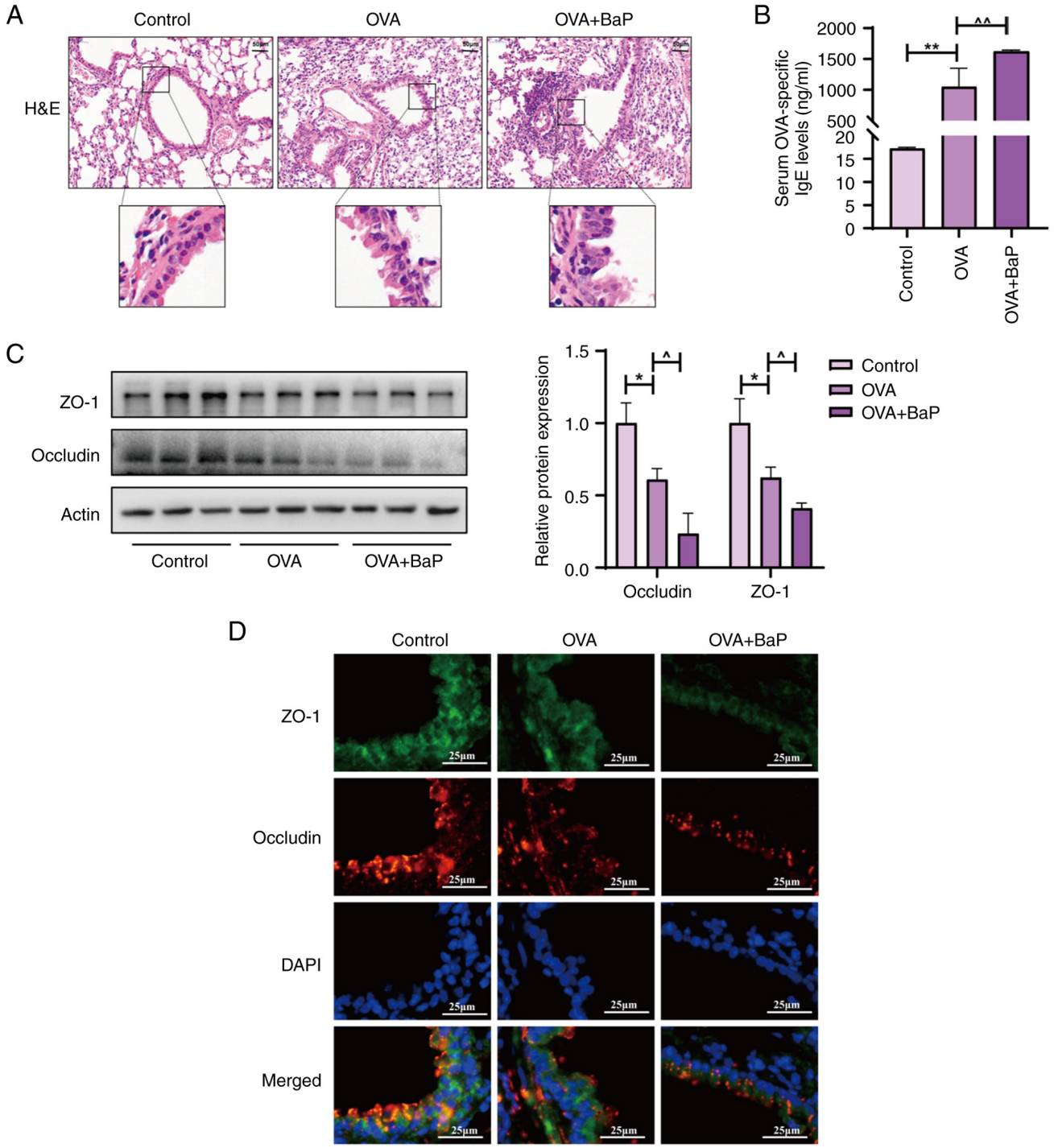

Figure 1. BaP can aggravate OVA-induced epithelial tight junction disruption in asthmatic mice. (A) Sample images of lung tissue stained with H&E from each group. Scale bar, 50 μm, magnification, x200, (n=6). (B) OVA-specific IgE serum levels were evaluated by ELISA (n=6). (C) The expression levels of occludin and ZO-1 were assessed using western blotting (n=3). (D) Sample images of lung tissue stained with immunofluorescence staining from each group. Scale bar, 25 μm (n=3). All data are presented as mean ± SD. *P<0.05, **P<0.01 vs. control group; $^{\wedge}$P<0.05, $^{\wedge\wedge}$P<0.01 vs. the OVA group. BaP, benzo[a]pyrene; OVA, ovalbumin; IgE, immunoglobulin E; ZO-1, zonula occludens-1; H&E, hematoxylin and eosin.

NLRP3 and ASC in 16HBE cells compared with the control, indicating elevated expression. Western blot analysis (Fig. 4B and C) further confirmed that BaP exposure upregulated NLRP3, ASC and caspase-1, leading to increased IL-18 and IL-1β levels, suggesting NLRP3 inflammasome activation.

BaP-induced ROS generation mediates NLRP3/caspase-1 signaling pathways in asthmatic mice. A crucial role is played by ROS in activating the NLRP3 inflammasome in bronchial epithelial cells, suggesting BaP may act by altering ROS production. Consequently, the present study investigated whether BaP can induce ROS generation. Elevated ROS level was demonstrated in the lung tissue of OVA-induced asthmatic mice after BaP exposure in Fig. 5A. To test this further, mice were treated with OVA + BaP, with or without NAC. The expression of NLRP3, ASC, caspase-1, IL-18 and IL-1β was

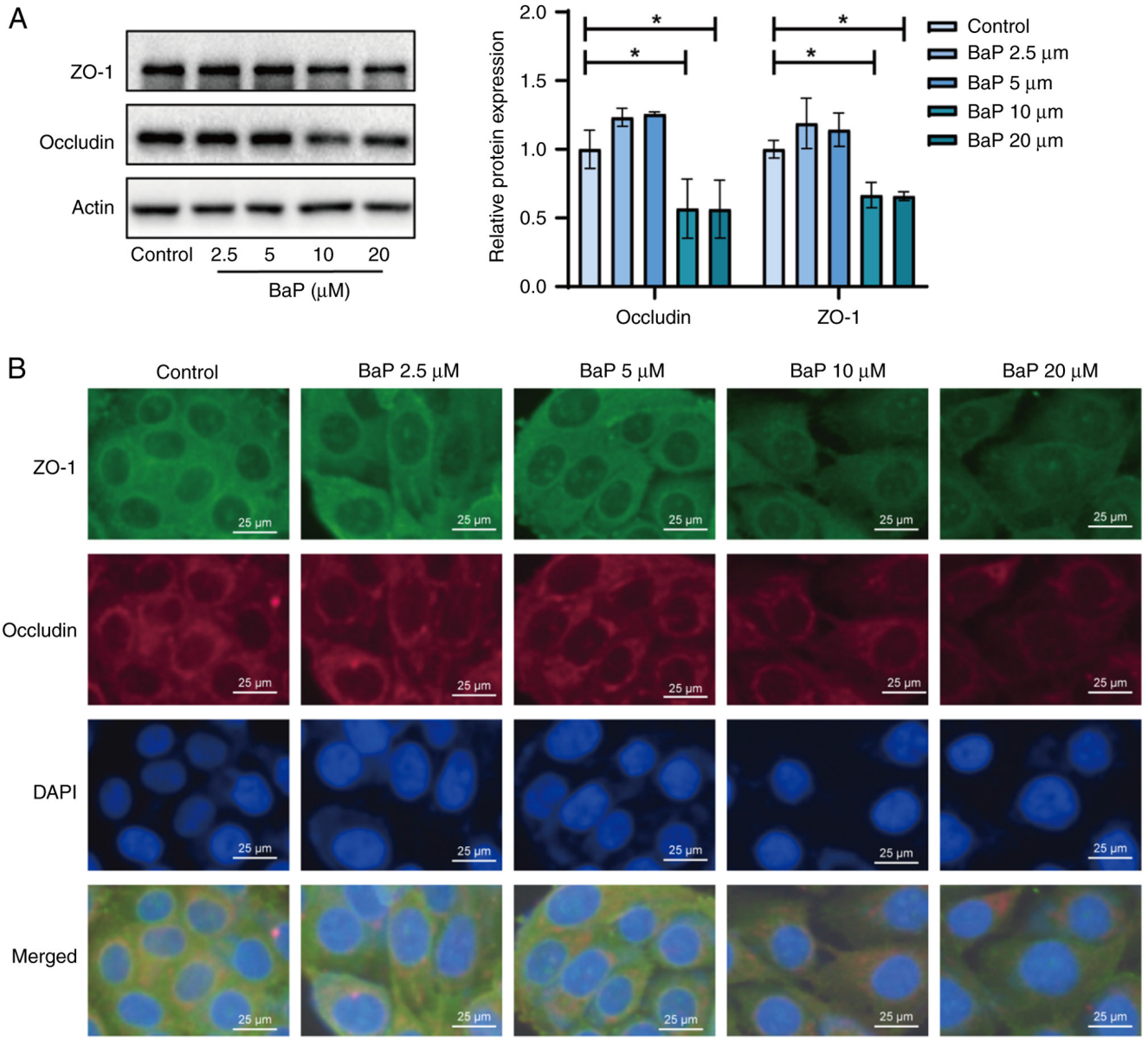

Figure 2. BaP can induce disruption of the tight junction of airway epithelial cells. (A) Western blot analysis of occludin and ZO-1 levels stimulated with different concentrations of BaP for 48 h in 16HBE cells (n=3). (B) Representative immunofluorescence staining images of occludin and ZO-1 in the 16HBE cells. Scale bar, 25 μm (n=3). All data are presented as mean ± SD. *P<0.05 vs. the control group. BaP, benzo[a]pyrene; ZO-1, zonula occludens-1; NLRP3, NOD-like receptor protein 3.

increased by BaP compared with the control, whereas NAC reduced their expression (Fig. 5B-D). These findings demonstrated that BaP-induced ROS activated the NLRP3/caspase-1 signaling pathway, which can be suppressed by ROS inhibition.

BaP-induced ROS generation mediates NLRP3/caspase-1 signaling pathways in airway epithelial cells. To explore this at a cellular level, ROS levels in 16HBE cells were assessed using the DCFH-DA probe, with fluorescence intensity reflecting ROS levels. Compared with the control group, BaP-treated cells revealed increased ROS, especially at 20 μM (Fig. 6A). In addition, the selection of a 20 μM concentration was based on its ability to markedly reduce the levels of tight junction proteins ZO-1 and occludin. This concentration falls within the commonly used range of 1-50 μM for studies examining similar mechanisms (26,27). NLRP3 and ASC expressions were elevated by BaP compared with the control group, which was reduced by NAC (Fig. 6B and C). Similarly, caspase-1, IL-18 and IL-1β expression followed the same trend (Fig. 6D), confirming that BaP-induced ROS could mediate NLRP3/caspase-1 pathway activation in airway epithelial cells.

BaP induces asthma epithelial tight junction disruption by increasing ROS generation. Exposure to air pollutants may elevate ROS production, a key mechanism underlying airway epithelial barrier dysfunction. The cytotoxic, mutagenic and highly lipophilic properties of BaP help in inducing oxidative damage through ROS. Elevated ROS levels increase epithelium permeability, while blocking ROS restore tight junction proteins such as occludin and ZO-1. As demonstrated

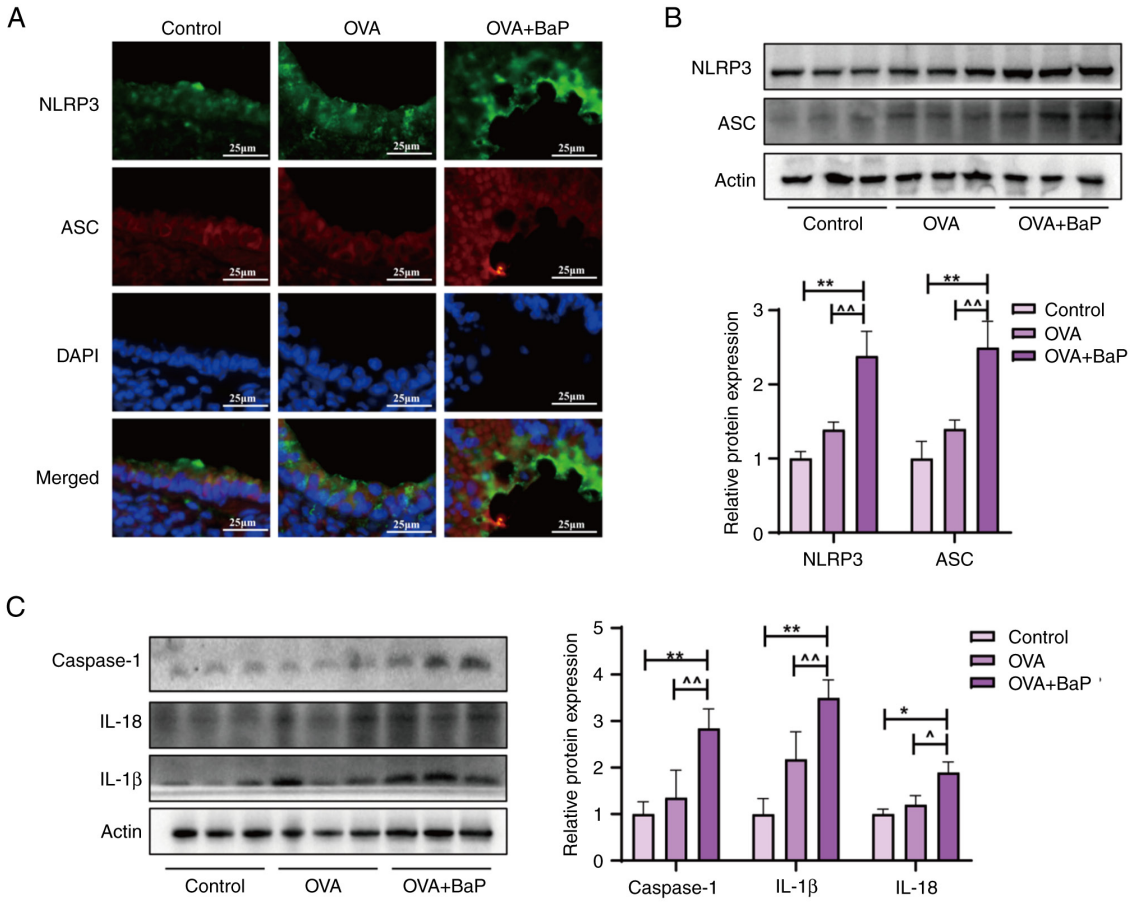

Figure 3. BaP induces NLRP3/caspase-1 pathway activation in lung tissue of asthmatic mice. (A) Representative immunofluorescence staining image for NLRP3 and ASC in mice lung tissue of each group. Scale bar, 25 μm. (B) Analysis of NLRP3 and ASC protein levels in mouse lung tissue using western blotting for each group (n=3). (C) Analysis of caspase-1, IL-18 and IL-1β levels in mouse lung tissue using western blotting for each group (n=3). All data are presented as mean ± SD. *P<0.05, **P<0.01 vs. the Control group; $^{\wedge}$P<0.05, $^{\wedge\wedge}$P<0.01 vs. the OVA group. BaP, benzo[a]pyrene; NLRP3, NOD-like receptor protein 3; ASC, apoptosis-associated speck-like protein containing a CARD; IL, interleukin; OVA, ovalbumin.

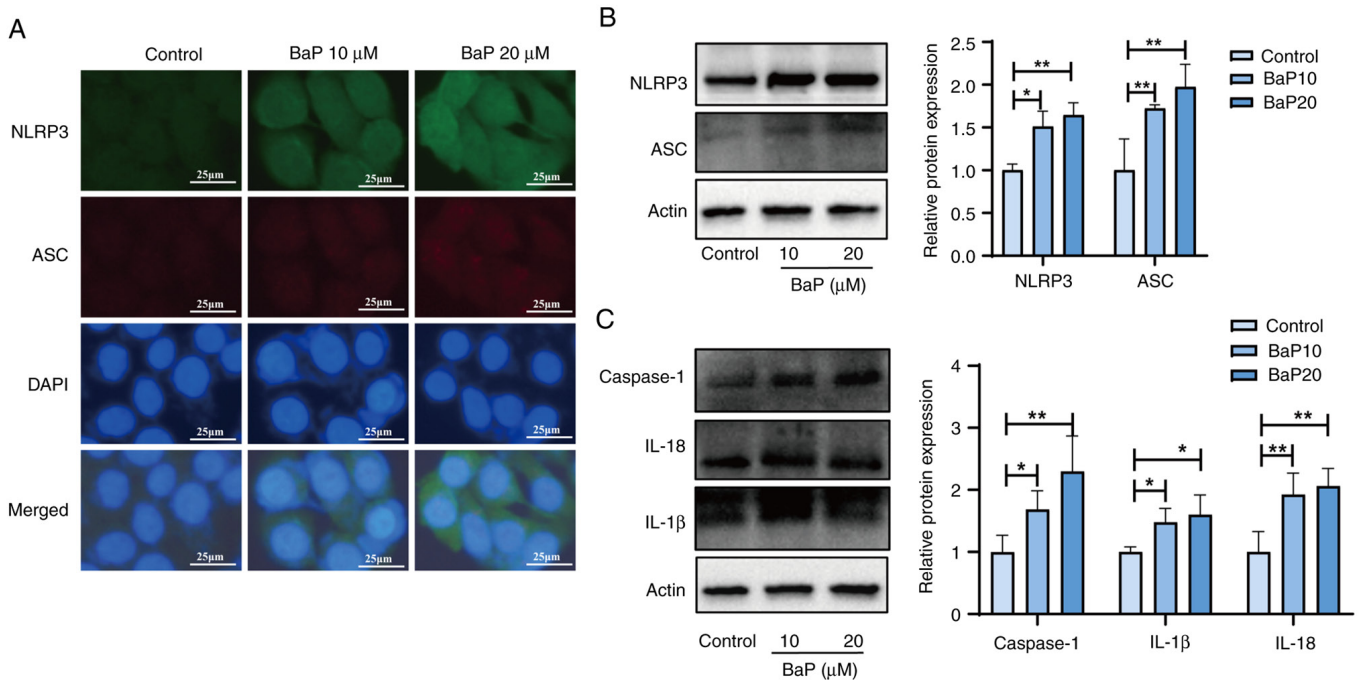

Figure 4. BaP activates the NLRP3/caspase-1 pathway in airway epithelial cells. (A) Representative immunofluorescence staining image for NLRP3 and ASC in 16HBE cells. Scale bar, 25 μm. (B) Western blot analysis of the protein levels of NLRP3 and ASC in 16HBE cells (n=3). (C) Western blot analysis of the protein levels of caspase-1, IL-18 and IL-1β in 16HBE cells (n=3). All data are presented as mean ± SD. *P<0.05, **P<0.01 vs. the control group. BaP, benzo[a] pyrene; NLRP3, NOD-like receptor protein 3; ASC, apoptosis-associated speck-like protein containing a CARD; IL, interleukin; NAC, N-acetylcysteine

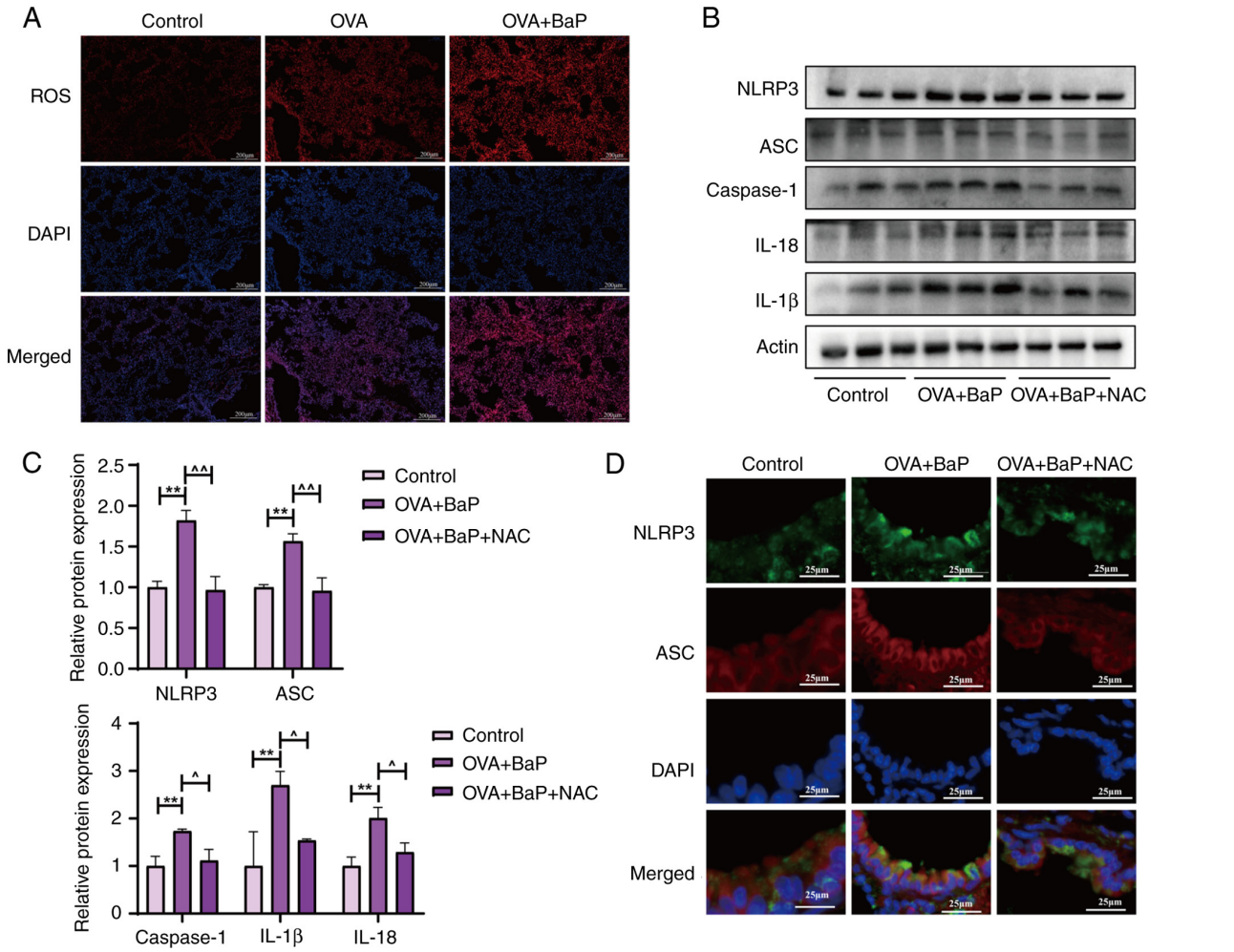

Figure 5. BaP-induced ROS generation mediates NLRP3/caspase-1 signaling pathways in asthmatic mice. (A) ROS level in mice lung tissue was determined via the ROS staining method in frozen lung tissue sections and observed with a fluorescence microscope. Scale bar, 200 μm (n=3). (B and C) Western blot analysis of the protein levels of NLRP3, ASC, caspase-1, IL-18 and IL-1β in mice lung tissue of each group (n=3). (D) Immunofluorescence staining images revealing NLRP3 and ASC in the lung tissues of mice across different groups. Scale bar, 25 μm (n=3). All data are presented as mean ± SD. **P<0.01 vs. the control group; $^{\wedge}$P<0.05, $^{\wedge\wedge}$P<0.01 vs. the OVA + BaP group. BaP, benzo[a]pyrene; ROS, reactive oxygen species; NLRP3, NOD-like receptor protein 3; IL, interleukin; NAC, N-acetylcysteine; ASC, apoptosis-associated speck-like protein containing a CARD; IL, interleukin; OVA, ovalbumin.

in Fig. 7A and B, ROS inhibitor NAC reduced ZO-1 and occludin in BaP-aggravated asthmatic mice. Meanwhile, NAC restored these proteins in BaP-treated 16HBE cells (Fig. 7C and D), suggesting that reducing ROS could alleviate BaP-induced airway barrier damage. This demonstrated that BaP disrupts the epithelial barrier in asthma by increasing ROS production.

BaP disrupts airway epithelial tight junctions through ROS-driven-NLRP3/caspase-1 signaling pathway. ROS-mediated NLRP3 signaling is a key molecular mechanism in tight and adherens junction disruption and airway epithelial barrier damage (28). Experimental results revealed that BaP markedly increases NLRP3 expression in 16HBE cells. The NLRP3 inhibitor MCC950 reversed the BaP-induced NLRP3 expression (Fig. 8A and B) and prevented the reduction of ZO-1 and occludin (Fig. 8C and D). Moreover, the ROS inhibitor NAC suppressed the BaP-induced NLRP3 expression. These results indicated that BaP disrupts airway epithelial barrier tight junctions through the ROS-driven NLRP3/caspase-1 signaling pathway.

Discussion

With advancing industrialization and urbanization, air pollution has become a growing concern and asthma incidence continues to rise yearly (29). Widespread environmental pollutants include PAHs, primarily originate from incomplete combustion of organic matter, such as forest fires, incineration and engine emission (30). Increased PAH exposure can lead to reduced lung function, potentially due to the production of ROS during PAH metabolism, which causes oxidative damage and disrupts respiratory barrier function. As one of the most toxic PAHs, BaP enhances airway hyperreactivity and lung inflammation in asthmatic mouse models co-exposed with the allergen Dermatophagoides farina 1, leading to elevated levels of epithelial cytokines such as thymic stromal lymphopoietin, IL-33 and IL-25 (31). Alone, BaP can induce oxidative stress, airway epithelial damage, lung toxicity and inflammation (32). It stimulates the airway by interfering with the forkhead box protein A2/IL-6/IL-6R/signal transducer and activator of the transcription 3 signaling pathway, promoting airway epithelial-mesenchymal transition (22).

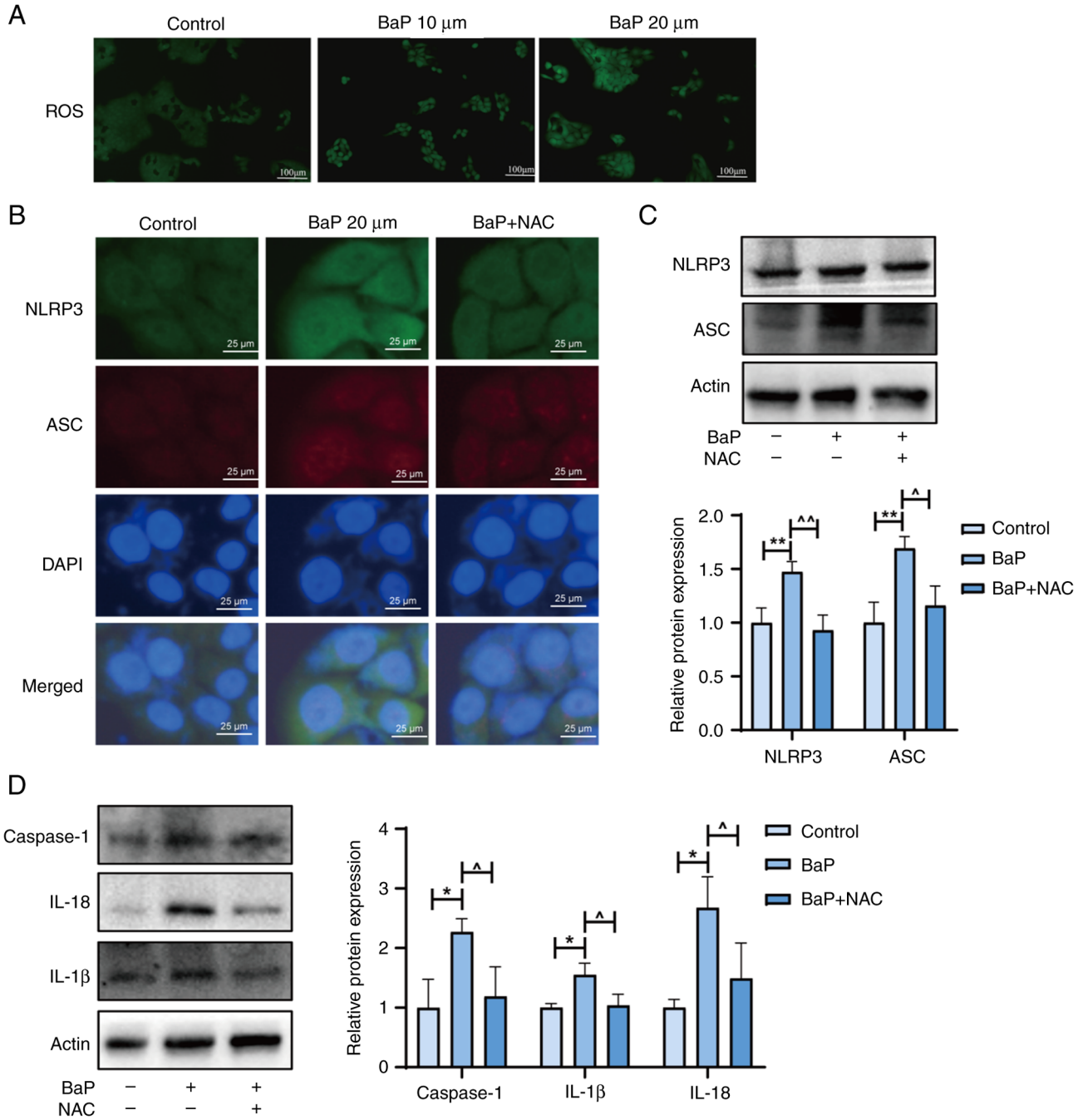

Figure 6. BaP-induced ROS generation mediates NLRP3/caspase-1 signaling pathways in airway epithelial cells. (A) ROS level in 16HBE cells was determined and observed with a fluorescence microscope. Scale bar, 25 μm (n=3). (B) Immunofluorescence staining images demonstrating NLRP3 and ASC in 16HBE cells. Scale bar, 25 μm (n=3). (C) Western blot analysis of the protein levels of NLRP3 and ASC in 16HBE cells of each group (n=3). (D) Western blot analysis of the protein levels of caspase-1, IL-18 and IL-1β in 16HBE cells (n=3). All data are presented as mean ± SD. *P<0.05, **P<0.01 vs. the control group; $^{\wedge}$P<0.05, $^{\wedge\wedge}$P<0.01 vs. the OVA + BaP group. BaP, benzo[a]pyrene; ROS, reactive oxygen species; NLRP3, NOD-like receptor protein 3; ASC, apoptosis-associated speck-like protein containing a CARD; IL, interleukin; NAC, N-acetylcysteine; IL, interleukin; OVA, ovalbumin..

According to Ni *et al* (33), BaP enhances the expression and activity of the cytochrome P450 1A1, leading to toxic effects on human airway epithelial cells through DNA damage and oxidative stress. The present study established an air pollution-exacerbated asthma mouse model with co-exposure to BaP and OVA. The results demonstrated that BaP and OVA co-exposure markedly increased inflammatory cell infiltration in lung tissue, caused more disorganized airway epithelial cell arrangement with partial detachment and led to more pronounced tracheal wall folding. These findings indicated that BaP exposure can exacerbate OVA-induced asthma and aggravate lung tissue damage.

Tight junctions are essential components of the airway epithelial barrier located at the apical region of epithelial cell connections. They are crucial for maintaining epithelial barrier integrity and polarity, forming the structural basis for the airway resistance to harmful substances. Disruption of airway epithelial integrity is a significant marker in asthma pathogenesis, with substantial evidence revealing airway epithelial cell shedding in bronchial biopsies from patients with

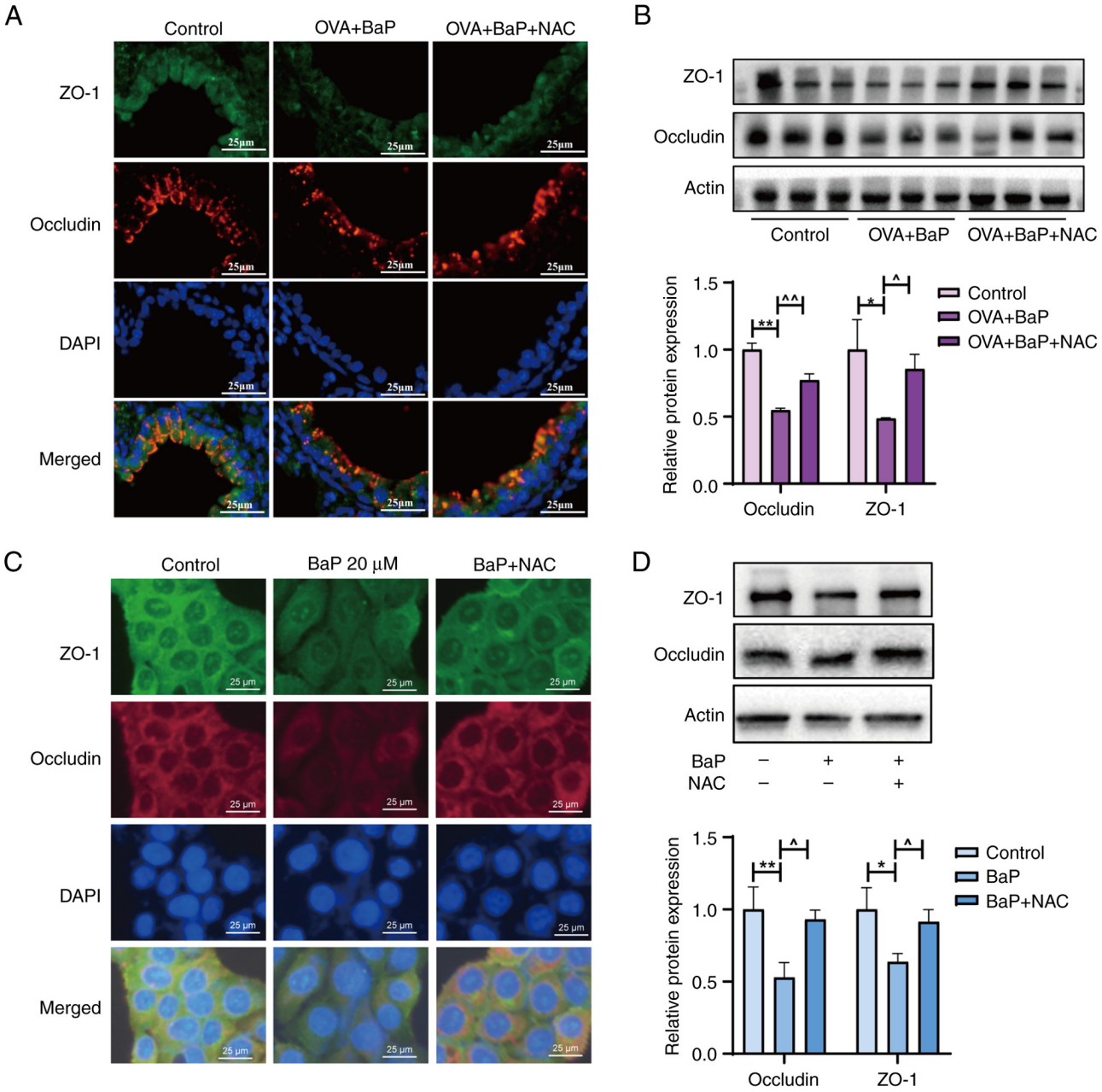

Figure 7. BaP induces asthma epithelial tight junction disruption by increasing ROS generation. (A) Representative immunofluorescence staining image for occludin and ZO-1 in mice lung tissue of each group. Scale bar, 25 μm (n=3). (B) Western blot analysis of the protein levels of occludin and ZO-1 in mice lung tissue of each group (n=3). (C) Representative immunofluorescence staining image for occludin and ZO-1 in 16HBE cells. Scale bar, 25 μm (n=3). (D) Western blot analysis of the protein levels of occludin and ZO-1 in 16HBE cells (n=3). All data are presented as mean ± SD. *P<0.05, **P<0.01 vs. the control group; $^{\wedge}$P<0.05, $^{\wedge\wedge}$P<0.01 vs. the BaP or OVA + BaP group. BaP, benzo[a]pyrene; ROS, reactive oxygen species; ZO-1, zonula occludens-1; NAC, N-acetylcysteine; OVA, ovalbumin.

varying asthma severity (34). Expression levels of Claudin-18, Claudin-4, Claudin-1 and ZO-1 are reduced in the bronchial epithelial cells of asthmatic patients (35). He *et al* (36) found that exposure to air pollutants such as particulate matter ≤2.5 μm ($PM_{2.5}$) decreases transcriptional and protein levels of tight junction markers E-cadherin, ZO-1 and occludin, exacerbating OVA-induced epithelial barrier damage. Diesel engine exhaust, a major urban pollutant, has been demonstrated both *in vitro* and *in vivo* to decrease transepithelial resistance and reduce ZO-1 and E-cadherin expression in airway epithelium (37,38). The present study investigated tight junction protein expression in lung tissues and airway epithelial cells of asthma mice induced by BaP, both *in vitro* and *in vivo*. Exposure to BaP suppressed ZO-1 and occludin expression in both asthmatic mice and 16HBE cells, leading to airway epithelial barrier disruption. This is the first study, to the best of the authors' knowledge, exploring the effect of BaP on the airway epithelial barrier in asthma. The findings further highlighted the toxic role of BaP in asthma pathogenesis, suggesting tight junctions as a promising target for mitigating barrier damage and its lasting impact on asthma. BaP is recognized as a ligand of aromatic hydrocarbon receptor (AHR) and is capable of activating AHR signaling, thereby influencing various cellular processes, including oxidative stress and

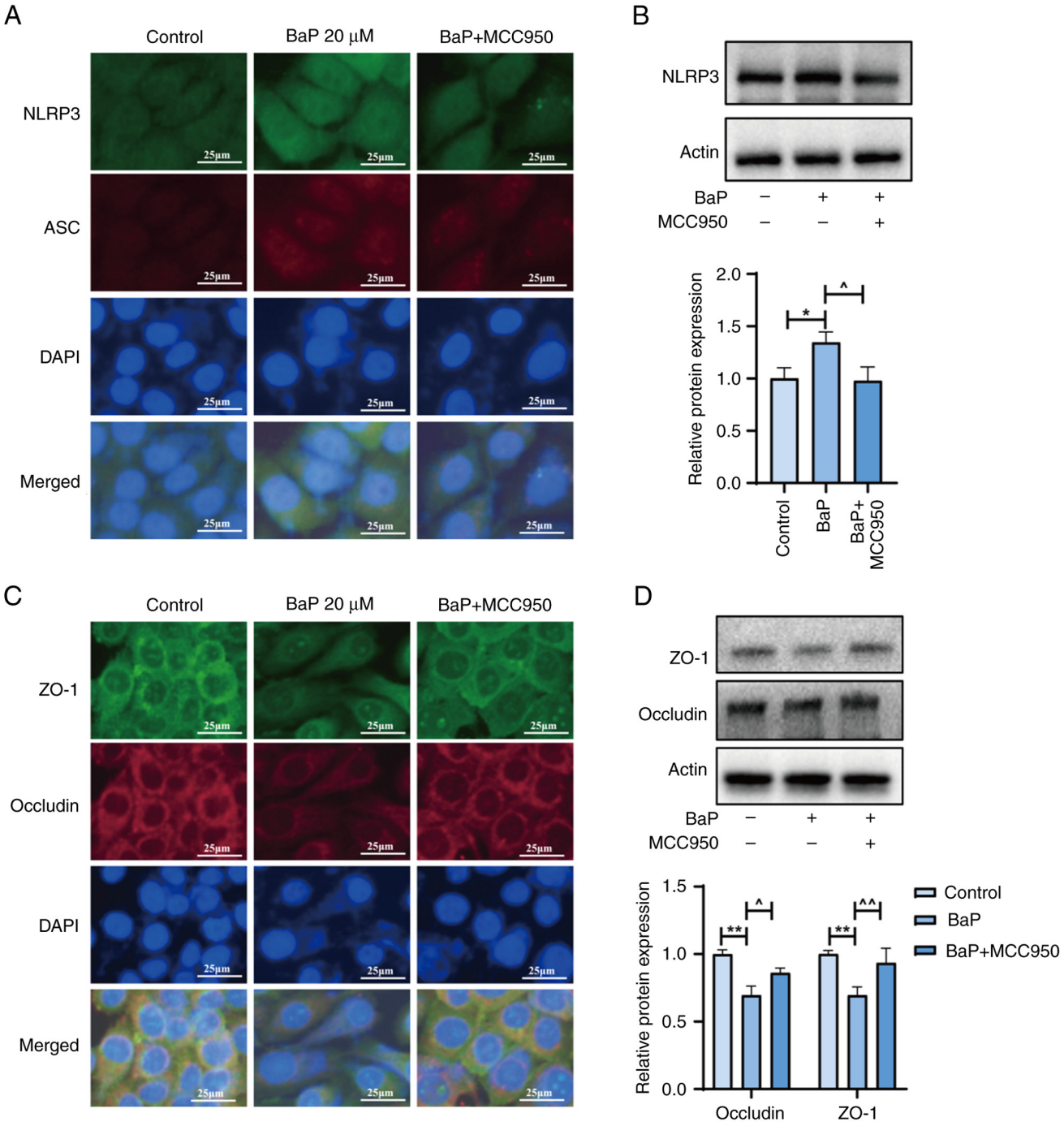

Figure 8. BaP disrupts airway epithelial tight junctions through ROS-driven-NLRP3/caspase-1 signaling pathway. (A) Representative immunofluorescence staining image for NLRP3 and ASC in 16HBE cells. Scale bar, 25 μm (n=3). (B) Western blot analysis of the protein levels of NLRP3 in 16HBE cells (n=3). (C) Representative immunofluorescence staining image for occludin and ZO-1 in 16HBE cells. Scale bar, 25 μm (n=3). (D) Western blot analysis of the protein levels of occludin and ZO-1 in 16HBE cells (n=3). All data are presented as mean ± SD. *P<0.05, **P<0.01 vs. the control group; $^{\wedge}$P<0.05, $^{\wedge\wedge}$P<0.01 vs. the BaP group. BaP, benzo[a]pyrene; ROS, reactive oxygen species; NLRP3, NOD-like receptor protein 3; ASC, apoptosis-associated speck-like protein containing a CARD; IL, interleukin; NAC, N-acetylcysteine.

inflammatory responses. Although the present study did not include experiments related to AHR, our previous research demonstrated the role of AHR in exacerbating asthma in mice exposed to BaP (23).

Research has demonstrated that NLRP3 inflammasome is vital for asthma development and progression, with two gain-of-function single-nucleotide polymorphisms in the NLRP3 gene linked to allergic asthma (39). NLRP3 inflammasome is an intracellular multiprotein complex consisting of NLRP3 receptor protein, the adaptor protein ASC and procaspase-1. Upon sensing external pathogens or danger signals, NLRP3 inflammasome cleaves procaspase-1 to activate caspase-1. Caspase-1 converts the pro IL-1β and IL-18 into active forms, facilitating their secretion (40,41). This cascade interferes with intercellular junctions, including tight and adherens junctions, compromising epithelial barrier integrity and function-processes closely tied to asthma onset and progression. In the present study, BaP-induced asthma mice

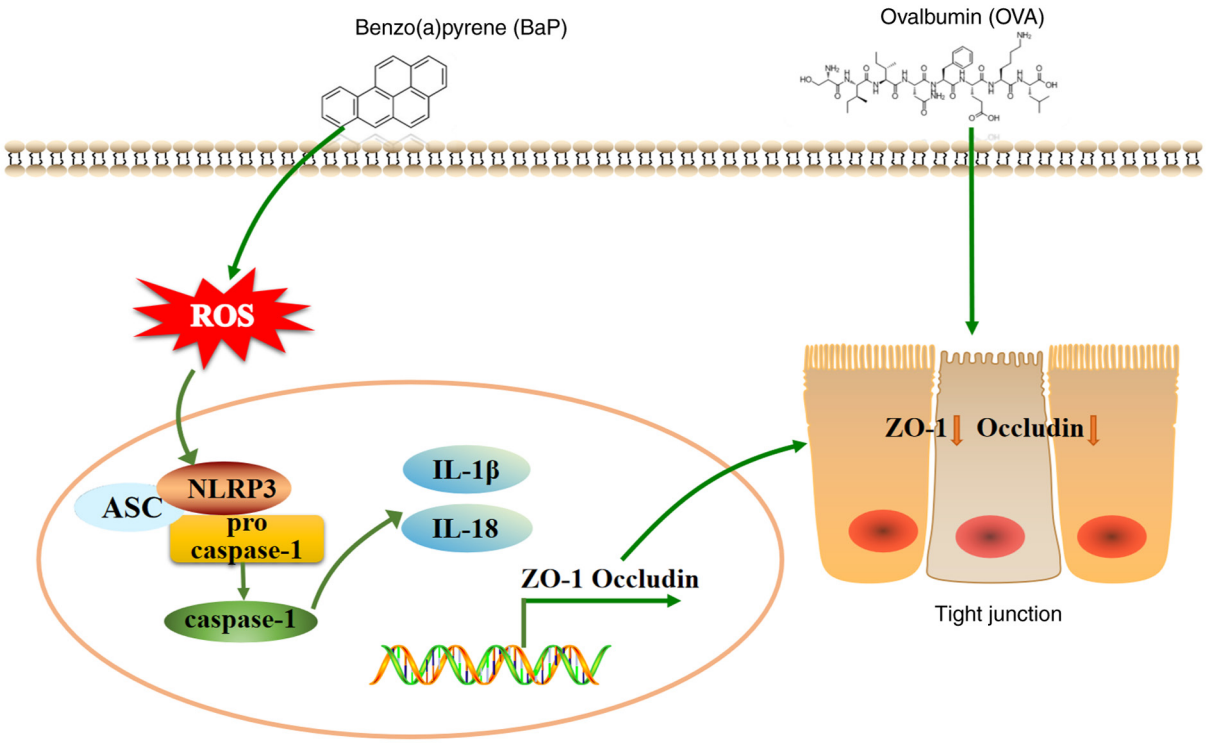

Figure 9. BaP aggravated OVA-induced epithelial tight junction disruption via ROS-driven NLRP3/caspase-1 signaling pathway in asthmatic mice. BaP, benzo[a]pyrene; OVA, ovalbumin; ROS, reactive oxygen species; NLRP3, NOD-like receptor protein 3; ASC, apoptosis-associated speck-like protein containing a CARD; IL, interleukin; ZO-1, zonula occludens-1.

and 16HBE cells exhibited activation of the NLRP3 inflammasome and downregulation of ZO-1 and occludin expression. Treatment with NLRP3 inhibitor MCC950 reversed the downregulation of ZO-1 and occludin, indicating that inhibiting NLRP3 activation can alleviate BaP-induced tight junction disruption. The NLRP3-IL-1β/IL-18 axis may regulate tight junction integrity through indirect signaling pathways.

Research indicates that ROS overproduction in the airways of individuals with asthma leads to oxidative stress and persistent inflammation (42). A crucial role is played by ROS in the activation of NLRP3 inflammasome in bronchial epithelial cells. Thioredoxin-interacting protein (TXNIP), a ligand for NLRP3, is reactive to ROS. Normally, the redox enzyme thioredoxin (TRX) binds to TXNIP and suppresses its activity (43). Elevated ROS levels cause dissociation of TRX-TXNIP, permitting TXNIP to connect with the leucine-rich repeat domain of NLRP3, thereby triggering inflammasome activation (44,45). Cytotoxicity, mutagenicity and high lipophilicity exhibited by BaP help it induce oxidative damage by generating ROS. The permeability of airway epithelium is increased by ROS and inhibiting ROS can restore the occludin and ZO-1 expression (46). It is hypothesized that BaP activates NLRP3 inflammasome by increasing ROS production, resulting in the downregulation of tight junction proteins and subsequent epithelial barrier disruption. In the present study, BaP exposure led to reduced expression of ZO-1 and occludin in asthma mice and 16HBE cells. Treatment with ROS inhibitor NAC not only restored ZO-1 and occludin levels but also inhibited the NLRP3 inflammasome activation. This indicates that inhibiting ROS can reduce airway barrier damage mediated by NLRP3-caspase-1.

In conclusion, the present study indicated that BaP impaired the airway epithelial barrier by downregulating the ZO-1 and occludin expression, with ROS playing a crucial role in BaP-induced airway epithelial barrier disruption. Furthermore, BaP appears to activate NLRP3 inflammasome through ROS generation. Mechanistically, the present study revealed a novel pathway in which ROS regulate NLRP3 inflammasome activation, leading to BaP-induced airway epithelial barrier disruption in asthma (Fig. 9).

However, the present study was subject to several limitations. The direct damage induced by cytokines or the indirect effects mediated by downstream inflammatory signals are not clear. Future research will aim to elucidate the regulation of tight junctions using IL-1 β/IL-18 neutralizing antibodies and receptor knockout models. It is also planned to employ conditional medium experiments to distinguish between direct and paracrine effects.

The OVA model is characterized by its strong immunogenicity and the immune response it induces closely parallels the immunopathological mechanisms observed in human asthma, with the added benefits of stability, reproducibility and low cost. However, although the OVA asthma model is mainly an acute model, it cannot accurately simulate the conditions of human asthma patients exposed to low concentrations of BaP over a long time. Future research should focus on developing a chronic exposure model to assess the generalizability of these findings.

Acknowledgements

Not applicable.

Funding

The present study was supported by Jiangsu Province Traditional Chinese medicine science and technology development program, grant no. MS2022053, the Postgraduate Research and Practice Innovation Program of Jiangsu Province, grant no. KYCX22_1940 and the Research Project Funding from Jiangning Chinese Medicine Hospital Affiliated to China Pharmaceutical University grant no. YJZD2025007.

Availability of data and materials

The data generated in the present study may be requested from the corresponding author.

Authors' contributions

YX and XX were responsible for writing the original draft, funding acquisition, data curation and conceptualization. YF and LW were responsible for formal analysis, data curation, investigation and data curation.LX and BW was responsible for supervision, project administration, investigation, writing-review and language editing.YX and BW confirm the authenticity of all the raw data. All authors read and approved the final manuscript.

Ethics approval and consent to participate

All animal procedures were approved by the Animal Ethics Committee of the Affiliated Hospital of Nanjing University of Traditional Chinese Medicine (approval no. 2022 DW-48-02).

Patient consent for publication

Not applicable.

Competing interests

The authors declare that they have no competing interests.

References:

1. Komlosi ZI, van de Veen W, Kovacs N, Szűcs G, Sokolowska M, O'Mahony L, Akdis M and Akdis CA: Cellular and molecular mechanisms of allergic asthma. Mol Aspects Med 85: 100995, 2022.
2. Huang K, Yang T, Xu J, Yang L, Zhao J, Zhang X, Bai C, Kang J, Ran P, Shen H, *et al*: Prevalence, risk factors, and management of asthma in China: A national cross-sectional study. Lancet 394: 407-418, 2019.
3. Bowatte G, Lodge CJ, Knibbs LD, Erbas B, Perret JL, Jalaludin B, Morgan GG, Bui DS, Giles GG, Hamilton GS, *et al*: Traffic related air pollution and development and persistence of asthma and low lung function. Environ Int 113: 170-176, 2018.
4. Hayakawa K, Tang N, Nagato E, Toriba A, Lin JM, Zhao L, Zhou Z, Qing W, Yang X, Mishukov V, *et al*: Long-Term trends in urban atmospheric polycyclic aromatic hydrocarbons and nitropolycyclic aromatic hydrocarbons: China, Russia, and Korea from 1999 to 2014. Int J Environ Res Public Health 17: 431, 2020.
5. Oliveira M, Slezakova K, Delerue-Matos C, Pereira MC and Morais S: Children environmental exposure to particulate matter and polycyclic aromatic hydrocarbons and biomonitoring in school environments: A review on indoor and outdoor exposure levels, major sources and health impacts. Environ Int 124: 180-204, 2019.
6. Honda A, Sawahara T, Hayashi T, Tsuji K, Fukushima W, Oishi M, Kitamura G, Kudo H, Ito S, Yoshida S, *et al*: Biological factor related to Asian sand dust particles contributes to the exacerbation of asthma. J Appl Toxicol 37: 583-590, 2017.
7. Choi H, Tabashidze N, Rossner P Jr, Dostal M, Pastorkova A, Kong SW, Gmuender H and Sram RJ: Altered vulnerability to asthma at various levels of ambient Benzo[a]Pyrene by CTLA4, STAT4 and CYP2E1 polymorphisms. Environ Pollut 231: 1134-1144, 2017.
8. Carrard J, Marquillies P, Pichavant M, Visez N, Lanone S, Tsicopoulos A, Chenivesse C, Scherpereel A and de Nadaï P: Chronic exposure to benzo (a)pyrene-coupled nanoparticles worsens inflammation in a mite-induced asthma mouse model. Allergy 76: 1562-1565, 2021.
9. Xiao C, Puddicombe SM, Field S, Haywood J, Broughton-Head V, Puxeddu I, Haitchi HM, Vernon-Wilson E, Sammut D, Bedke N, *et al*: Defective epithelial barrier function in asthma. J Allergy Clin Immunol 128: 549-56.e1-12, 2011.
10. Aghapour M, Ubags ND, Bruder D, Hiemstra PS, Sidhaye V, Rezaee F and Heijink IH: Role of air pollutants in airway epithelial barrier dysfunction in asthma and COPD. Eur Respir Rev 31: 210112, 2022
11. Song Y, Fu W, Zhang Y, Huang D, Wu J, Tong S, Zhong M, Cao H and Wang B: Azithromycin ameliorated cigarette smoke-induced airway epithelial barrier dysfunction by activating Nrf2/GCL/GSH signaling pathway. Respir Res 24: 69, 2023.
12. Garcia MA, Nelson WJ and Chavez N: Cell-Cell junctions organize structural and signaling networks. Cold Spring Harb Perspect Biol 10: a029181, 2018.
13. Rusu AD and Georgiou M: The multifarious regulation of the apical junctional complex. Open Biol 10: 190278, 2020.
14. Tao Y, Wang Y, Wang X, Wang C, Bao K, Ji L, Jiang G and Hong M: Calycosin suppresses epithelial derived initiative key factors and maintains epithelial barrier in allergic inflammation via TLR4 mediated NF-κB pathway. Cell Physiol Biochem 44: 1106-1119, 2017.
15. Tsukita S, Furuse M and Itoh M: Multifunctional strands in tight junctions. Nat Rev Mol Cell Biol 2: 285-293, 2001.
16. Kang DH, Lee TJ, Kim JW, Shin YS, Kim JD, Ryu SW, Ryu S, Choi YH, Kim CH, You E, *et al*: Down-regulation of diesel particulate matter-induced airway inflammation by the PDZ motif peptide of ZO-1. J Cell Mol Med 24: 12211-12218, 2020.
17. Campbell HK, Maiers JL and DeMali KA: Interplay between tight junctions & adherens junctions. Exp Cell Res 358: 39-44, 2017.
18. Chiba T, Uchi H, Tsuji G, Gondo H, Moroi Y and Furue M: Arylhydrocarbon receptor (AhR) activation in airway epithelial cells induces MUC5AC via reactive oxygen species (ROS) production. Pulm Pharmacol Ther 24: 133-140, 2011.
19. Zhang L, He X, Xiong Y, Ran Q, Xiong A, Wang J, Wu D, Niu B and Li G: Transcriptome-wide profiling discover: PM2.5 aggravates airway dysfunction through epithelial barrier damage regulated by Stanniocalcin 2 in an OVA-induced model. Ecotoxicol Environ Saf 220: 112408, 2021.
20. Chen M, Yang T, Meng X and Sun T: Azithromycin attenuates cigarette smoke extract-induced oxidative stress injury in human alveolar epithelial cells. Mol Med Rep 11: 3414-3422, 2015.
21. Li L, Bao B, Chai X, Chen X, Su X, Feng S and Zhu X: The anti-inflammatory effect of callicarpa nudiflora extract on H. Pylori-infected GES-1 cells through the inhibition of ROS/NLRP3/Caspase-1/IL-1β signaling axis. Can J Infect Dis Med Microbiol 2022: 5469236, 2022.
22. Tang L, Chen B, Wang B, Xu J, Yan H, Shan Y and Zhao X: Mediation of FOXA2/IL-6/IL-6R/STAT3 signaling pathway mediates benzo[a]pyrene-induced airway epithelial mesenchymal transformation in asthma. Environ Pollut 357: 124384, 2024.
23. Wang B, Tang L, Sun X, Zhang Q, Liu CY, Zhang XN, Yu KY, Yang Y, Hu J, Shi XL, *et al*: Qufeng Xuanbi formula inhibited benzo[a]pyrene-induced aggravated asthma airway mucus secretion by AhR/ROS/ERK pathway. J Ethnopharmacol 319: 117203, 2024.
24. Fang R, Cheng Y, Chen P, Hu J and Yang LQ: PGC-1α agonist ZLN005 ameliorates OVA-induced asthma in BALB/c mice through modulating the NF-κB-p65/NLRP3 pathway. Iran J Basic Med Sci 28: 710-717, 2025.
25. Zhang YY, Jiang YY, Zhang DM, Hu X, Deng S, Li X and Feng J: Role of GLCCI1 in inhibiting PI3K-induced NLRP3 inflammasome activation in asthma. Chin Med J Pulm Crit Care Med 2: 279-288, 2024.

26. Cui X, Mi T, Xiao X, Dong Y, Zhang H, Chen G and Gu X: Metabolomic reprogramming induced by Benzo[a]pyene in skin keratinocytes and protective effects of glutathione amino acid precursors. J Cosmet Dermatol 24: e70168, 2025.
27. Siangcham T, Vivithanaporn P, Jantakee K, Ruangtong J, Thongsepee N, Martviset P, Chantree P, Sornchuer P and Sangpairoj K: Impact of benzo (a)pyrene and pyrene exposure on activating autophagy and correlation with endoplasmic reticulum stress in human astrocytes. Int J Mol Sci 26: 1748, 2025.
28. Shen C, Luo Z, Ma S, Yu C, Lai T, Tang S, Zhang H, Zhang J, Xu W and Xu J: Microbe-Derived antioxidants protect IPEC-1 cells from H2O2-induced oxidative stress, inflammation and tight junction protein disruption via activating the Nrf2 pathway to inhibit the ROS/NLRP3/IL-1β signaling pathway. Antioxidants (Basel) 13: 533, 2024.
29. Kampa M and Castanas E: Human health effects of air pollution. Environ Pollut 151: 362-367, 2008.
30. Padilla-Garfias F, Araiza-Villanueva M, Calahorra M, Sánchez NS and Peña A: Advances in the degradation of polycyclic aromatic hydrocarbons by yeasts: A review. Microorganisms 12: 2484, 2024.
31. Wang E, Liu X, Tu W, Do DC, Yu H, Yang L, Zhou Y, Xu D, Huang SK, Yang P, *et al*: Benzo (a)pyrene facilitates dermatophagoides group 1 (Der f 1)-induced epithelial cytokine release through aryl hydrocarbon receptor in asthma. Allergy 74: 1675-1690, 2019
32. Qamar W, Khan R, Khan AQ, Rehman MU, Lateef A, Tahir M, Ali F and Sultana S: Alleviation of lung injury by glycyrrhizic acid in benzo (a)pyrene exposed rats: Probable role of soluble epoxide hydrolase and thioredoxin reductase. Toxicology 291: 25-31, 2012.
33. Ni Z, Ma H, Li X, Zou L, Liu Z, Wang X, Ma H and Yang L: Wogonin alleviates BaP-induced DNA damage and oxidative stress in human airway epithelial cells by dual inhibiting CYP1A1 activity and expression. Environ Toxicol 38: 2717-2729, 2023.
34. Martinez-Giron R and van Woerden HC: Disruption of airway epithelium in asthma pathogenesis: Are protozoa responsible? Proc Am Thorac Soc 7: 161, 2010.
35. Loxham M and Davies DE: Phenotypic and genetic aspects of epithelial barrier function in asthmatic patients. J Allergy Clin Immunol 139: 1736-1751, 2017.
36. He X, Zhang L, Hu L, Liu S, Xiong A, Wang J, Xiong Y and Li G: PM2.5 aggravated OVA-induced epithelial tight junction disruption through fas associated via death domain-dependent apoptosis in asthmatic mice. J Asthma Allergy 14: 1411-1423, 2021.
37. Fukuoka A, Matsushita K, Morikawa T, Takano H and Yoshimoto T: Diesel exhaust particles exacerbate allergic rhinitis in mice by disrupting the nasal epithelial barrier. Clin Exp Allergy 46: 142-152, 2016.
38. Zarcone MC, Duistermaat E, van Schadewijk A, Jedynska A, Hiemstra PS and Kooter IM: Cellular response of mucociliary differentiated primary bronchial epithelial cells to diesel exhaust. Am J Physiol Lung Cell Mol Physiol 311: L111-L123, 2016.
39. Hitomi Y, Ebisawa M, Tomikawa M, Imai T, Komata T, Hirota T, Harada M, Sakashita M, Suzuki Y, Shimojo N, *et al*: Associations of functional NLRP3 polymorphisms with susceptibility to food-induced anaphylaxis and aspirin-induced asthma. J Allergy Clin Immunol 124: 779-785.e6, 2009.
40. Sharma M and de Alba E: Structure, activation and regulation of NLRP3 and AIM2 inflammasomes. Int J Mol Sci 22: 872, 2021
41. Christgen S, Place DE and Kanneganti T: Toward targeting inflammasomes: Insights into their regulation and activation. Cell Res 30: 315-327, 2020.
42. He W, Rahman MH, Bajgai J, Abdul-Nasir S, Mo C, Ma H, Goh SH, Bomi K, Jung H, Kim CS, *et al*: Hydrogen gas inhalation alleviates airway inflammation and oxidative stress on ovalbumin-induced asthmatic BALB/c mouse model. Antioxidants (Basel) 13: 1328, 2024.
43. Zhang X, Zhang J, Chen X, Hu QH, Wang MX, Jin R, Zhang QY, Wang W, Wang R, Kang LL, *et al*: Reactive oxygen species-induced TXNIP drives fructose-mediated hepatic inflammation and lipid accumulation through NLRP3 inflammasome activation. Antioxid Redox Signal 22: 848-870, 2015.
44. Zhou D, Cai L, Xu J, Fu D, Yan L and Xie L: Exploring the mitigating potential of anthocyanin Malvidin in a mouse model of bleomycin-induced pulmonary fibrosis by inhibiting NLRP3 inflammasome activation and oxidative stress. J Inflamm (Lond) 22: 14, 2025.
45. Wang Y, Wang J, Chen Y, Li X and Jiang Z: Decursinol angelate relieves inflammatory bowel disease by inhibiting the ROS/TXNIP/NLRP3 pathway and pyroptosis. Front Pharmacol 15: 1520040, 2024.
46. Zhang X, Gu L, Chen Y, Wang T and Xing H: L-selenomethionine inhibits small intestinal ferroptosis caused by ammonia exposure through regulating ROS-mediated iron metabolism. Ecotoxicol Environ Saf 289: 117477, 2024.